Killer cell immunoglobulin-like receptor 3DL1 variation modifies HLA-B*57 protection against HIV-1

Maureen P. Martin[1*], Vivek Naranbhai[2,3*], Patrick R. Shea[4], Ying Qi[1], Veron Ramsuran[1,3,5], Nicolas Vince[1,6,7], Xiaojiang Gao[1], Rasmi Thomas[8,9], Zabrina L. Brumme[10,11], Jonathan M. Carlson[12], Steven M. Wolinsky[13], James J. Goedert[14], Bruce D. Walker[2], Florencia P. Segal[15], Steven G. Deeks[16], David Haas[17], Stephen A. Migueles[18], Mark Connors[18], Nelson Michael[8,9], Jacques Fellay[19], Emma Gostick[20], Sian Llewellyn-Lacey[20], David A. Price[20], Bernard A. Lafont[21], Phillip Pymm[22], Philippa M Saunders[23], Jacqueline Widjaja[23], Shu Cheng Wong[23], Julian P. Vivian[22], Jamie Rossjohn[20,22], Andrew G. Brooks[23], Mary Carrington[1,2*]

[1]Cancer and Inflammation Program, Leidos Biomedical Research Inc., Frederick National Laboratory for Cancer Research, Frederick, MD, USA; [2]Ragon Institute of MGH, MIT and Harvard, Boston, MA, USA; [3]Centre for the AIDS Programme of Research in South Africa (CAPRISA), University of KwaZulu-Natal, Durban, South Africa; [4]Institute for Genomic Medicine, Columbia University, New York, NY, USA; [5]KwaZulu-Natal Research Innovation and Sequencing Platform (KRISP), School of Laboratory Medicine and Medical Sciences, University of KwaZulu-Natal, Durban, South Africa; [6]ATIP-Avenir, Centre de Recherche en Transplantation et Immunologie UMR 1064, INSERM, Université de Nantes, Nantes, France; [7]Institut de Transplantation Urologie Néphrologie (ITUN), CHU Nantes, Nantes, France; [8]U.S. Military HIV Research Program, Walter Reed Army Institute of Research, Silver Spring, MD, USA; [9]Henry M. Jackson Foundation for the Advancement of Military Medicine, Bethesda, MD, USA; [10]Faculty of Health Sciences, Simon Fraser University, Burnaby, B.C., Canada; [11]British Columbia Centre for Excellence in HIV/AIDS, Vancouver, B.C., Canada; [12]Microsoft Research, Redmond, WA, USA; [13]Division of Infectious Diseases, Northwestern University Feinberg School of Medicine, Chicago, IL, USA; [14]Infections and Immunoepidemiology Branch, Division of Cancer Epidemiology and Genetics, National Cancer Institute, National Institutes of Health, Bethesda, MD, USA; [15]Brigham and Women's Hospital, Boston, MA, USA; [16]San Francisco General Hospital Medical Center, San Francisco, CA, USA; [17]Vanderbilt University School of Medicine, Nashville, TN, USA; [18]Laboratory of Immunoregulation, National Institute of Allergy and Infectious Diseases, National Institutes of Health, Bethesda, MD, USA; [19]School of Life Sciences, Swiss Federal Institute of Technology, Lausanne, Switzerland; [20]Cardiff University School of Medicine, Heath Park, University Hospital of Wales, Cardiff, UK; Non-Human Primate Immunogenetics and Cellular Immunology Unit, [21]Viral Immunology section, Office of the Scientific Director, National Institute of Allergy and Infectious Diseases, National Institutes of Health, Bethesda, MD, USA; [22]Infection and Immunity Program and Department of Biochemistry and Molecular Biology, Biomedicine Discovery Institute, and Australian Research Council Centre of Excellence in Advanced Molecular Imaging, Monash University, Clayton, Victoria, Australia; [23]Department of Microbiology and

Immunology, Peter Doherty Institute for Infection and Immunity, The University of Melbourne, Parkville, Victoria, Australia.

*These authors contributed equally.

Corresponding Author: Mary Carrington, P.O. Box B, Bldg. 560, Rm 21-89, Frederick, MD 21702.
Tel. 301-846-1390.
Email: carringm@mail.nih.gov

Conflict of interest statement: The authors have declared that no conflict of interest exists.

Abstract

HLA-B*57 control of HIV involves enhanced CD8+ T cell responses against infected cells, but extensive heterogeneity exists in level of HIV control among B*57+ individuals. Using whole genome sequencing of untreated B*57+ HIV-1 infected controllers and non-controllers, we identified a single variant (rs643347A/G) encoding an isoleucine to valine substitution at position 47 (I47V) of the inhibitory killer cell immunoglobulin-like receptor, KIR3DL1, as the only significant modifier of B*57 protection. The association replicated in an independent cohort and across multiple outcomes. The modifying effect of I47V was confined to B*57:01, and was not observed for the closely related B*57:03. Positions 2, 47, and 54 track one another nearly perfectly, and two KIR3DL1 allotypes differing only at these three positions showed significant differences in binding B*57:01 tetramers, where the protective allotype showed lower binding. Thus, variation in an immune natural killer cell receptor that binds B*57:01 modifies its protection. These data speak to exquisite specificity of KIR-HLA interactions in human health and disease.

Introduction

HIV-1 disease progression is influenced by host genetic factors and varies greatly among infected individuals. Polymorphism in the *HLA* class I locus has been consistently shown to associate with outcome of untreated HIV-1 infection by both the candidate gene approach (1) and genome-wide association studies (2, 3). The influence of *HLA-B* alleles is particularly robust, among which *HLA-B*57* and *-B*27* exhibit consistent protective effects (4-8) and *HLA-B*35* subtypes associate with accelerated disease progression (9). *B*57* is highly enriched in rare individuals who maintain undetectable viral loads (VL, plasma HIV-1 RNA <50 copies/mL) in the absence of antiretroviral therapy (10). Up to 50% of these "elite controllers" carry *B*57* alleles as compared to a frequency of 7-8% in non-controllers (11) or the general Caucasian population. Notably, however, in the absence of antiretroviral therapy, most *B*57*+ HIV infected individuals fail to control HIV and typically progress to AIDS with a temporal range similar to those without *B*57* (8), indicating the presence of distinct modifiers of *B*57* protection.

The mechanistic role of *HLA-B*57* in control of the virus is not fully understood, but data suggest that immune responses mediated through both acquired and innate mechanisms are involved. B*57 binds several immunodominant epitopes located in conserved regions of Gag, implicating B*57-restricted CD8+ T-cell responses in controlling viral replication (12-14). Escape mutations within these B*57-restricted epitopes can result in reduced viral fitness (15-19). Viral adaptation to host *HLA* genotypes results in escape

from cytotoxic T lymphocyte (CTL) responses, and high levels of adaptation appear to have profound deleterious effects on viral control, even among *B*57*+ individuals (20). Reduced viral fitness does not compensate for the loss of an effective CTL response, and HIV controllers with *B*57* have significantly lower adaptation scores compared to *B*57* non-controllers. Nevertheless, CTL from patients with *B*57* are more cross-reactive to various HIV epitopes after point mutations in these epitopes have occurred relative to CTLs from patients with *B*08*, an allele that associates with more rapid disease progression (21). This observation is supported by computational modeling of thymic selection in which a larger fraction of the naïve repertoire of B*57-restricted T-cell clones is specific for HIV relative to that of other alleles, and B*57-restricted T cells are more cross-reactive to mutants of targeted epitopes (22), possibly impeding viral adaptation in *B*57*+ individuals.

Here we identify a nonsynonymous variant in the *KIR3DL1* gene (I47V) that modifies *B*57* protection against HIV-1. This is the only locus identified genome-wide to associate with level of *B*57* control, and the effect replicates in an independent cohort of *B*57*+ HIV-1-infected subjects. The protective effect of I47V was restricted to the *B*57:01* subtype and no such effect was observed for the closely related *B*57:03*. These two allotypes differ only at positions 114 and 116 located in the E and F pockets, respectively, which specify peptide binding, suggesting that differences in positioning or sequence of peptides bound to B*57 are in part responsible for the protective effect of KIR3DL1 47V.

Results

The *KIR3DL1* rs*643347G* variant is enriched in *B*57*+ HIV-1 infected controllers

We performed whole genome sequencing (WGS) of *B*57*+ controllers (n = 100) and *B*57*+ non-controllers (n = 100) (Supplemental Table 1) in order to identify host genetic modifiers of *B*57* control of HIV-1. The controller group used in the whole genome study was highly enriched for elite controllers (89% with viral load <500 copies/ml). Sequence data was of high quality for 187 samples, including 97 controllers and 90 non-controllers, allowing for statistical analysis of 56,808 variants genome-wide that were chosen based on predicted functional consequences (e.g. nonsynonymous, splice site acceptor/donor, start/stop loss or gain, frameshift variants). Only a single variant, *rs643347A/G*, located in the *KIR3DL1* gene remained statistically significant after Bonferroni correction for multiple testing (Supplemental Figure 1). This variant results in an isoleucine (*rs643347A*) to valine (*rs643347G*) amino acid (aa) substitution at codon 47 within the D0 domain of the mature KIR3DL1 protein, and *rs643347G* associated with elite control ($p = 2.4 \times 10^{-7}$, Fisher's exact test; Table 1). Two additional variants within the *KIR* genomic region, *rs1049150* (isoleucine to leucine at aa54 in KIR3DL1) and *rs1049215* (threonine to alanine at aa115 in KIR2DL4), both of which are in linkage disequilibrium (LD) with *rs643347* ($r^2 = 0.93$, D' = 1, and $r^2 = 0.76$, D' = 0.99, respectively), were also identified, but these did not remain statistically significant after correction (Supplemental Figure 1).

In order to validate the WGS results, we analyzed data from an independent *B*57*+ cohort comprised of 297 HIV+ individuals with a more lenient definition of control (VL < 2000 viral RNA copies/ml of plasma) and 213 non-controllers (VL > 10,000 viral RNA copies/ml of plasma) (Supplemental Table 1). This cohort had a broader range of clinical phenotypes relative to the extreme phenotypes of the initial cohort in which WGS was performed, particularly with respect to the controllers (89% “elite” controllers in the WGS cohort vs <60% in the validation cohort, where elite control is defined as having undetectable viral loads using standard assays). *KIR3DL1* subtyping was performed in the validation cohort and confirmed the association of 47V with significantly better HIV control (56.9% in controllers vs. 47.7% in non-controllers; p = 0.004; Table 1). The weaker effect observed in the validation cohort is consistent with the broader range of clinical phenotypes in this cohort relative to the discovery cohort.

Variants encoding amino acids 2, 47, and 54 have the strongest effects on HIV-1 control relative to other *KIR3DL1* nonsynonymous variants

KIR3DL1 is a highly polymorphic locus, containing many nonsynonymous variants (http://www.ebi.ac.uk/ipd/kir/) that are in strong LD with one another. While WGS pointed to aa47 as having the greatest effect on *B*57* control of HIV-1, other variants within the gene that may not have reached genome-wide significance due to poor detection quality could contribute to the effect observed with aa47. We therefore used the pooled data from the WGS and validation

cohorts to test for effects of each nonsynonymous variant within the *KIR3DL1* gene. Homozygotes plus heterozygotes of the lower frequency allele were compared to homozygotes of the higher frequency allele in order to gain power when testing rarer allelic variants. Variants encoding aa positions 2, 47, and 54 are in strong LD (23) (Supplemental Table 2) and thus, the effect of each of these 3 amino acids was comparable (OR = 0.2-0.3, p = 0.003-0.0003). Amino acid 283 showed a weak effect (OR = 0.6, p = 0.02), but no other amino acid variant in the KIR3DL1 molecule significantly modified the effect of *B*57* on HIV control (data not shown). Thus, I47V tags two additional coding variants and although I47V appears the most statistically robust, any one or combination of the three amino acid variants at positions 2, 47, and 54 may be responsible for modulating *B*57* protection against HIV-1.

Genotypes encoding KIR3DL1 amino acid 47 (I47V) act in a co-dominant fashion to impact *HLA-B*57* control of HIV-1

Our initial analyses of I47V considered allelic (rather than genotypic) frequencies of 47I vs 47V (Table 1), and samples carrying only one functional copy of *KIR3DL1* (i.e. those who carry on the other haplotype either the activating *KIR3DS1,* or *KIR3DL1*004,* an allele that is not expressed on the cell surface) or no copies of functional *KIR3DL1* were included in the analyses. *KIR3DL1* allele frequencies are shown in Supplemental Figure 2 and Supplemental Table 3. As KIR3DL1*004 does not bind B*57 expressed on target cells (24, 25), this allele should be functionally irrelevant in the analyses performed herein. Furthermore,

both *KIR3DS1* and *KIR3DL1*004* may actually confound our results since both have been associated with protection in HIV cohorts previously (albeit not in combination with *B*57* specifically) (26, 27). In order to eliminate any potential confounding effect of *KIR3DS1* and *KIR3DL1*004* on modulation of *B*57* protection against HIV, we excluded subjects with these two alleles and limited the genotypic analyses to subjects with two copies of *KIR3DL1* (i.e. those with only a single copy or >2 copies of *KIR3DL1* were excluded), since variable gene copy number may also influence our analysis (28). The three strict genotypes of I47V (i.e. VV, IV, and II) were then tested for their frequencies among controllers (mVL<2000 viral RNA copies/ml plasma) as compared to non-controllers (mVL>10,000 viral RNA copies/ml plasma), all of whom were *B*57*+ (Supplemental Table 1). The 47VV genotype was strongly associated with protection relative to 47II (OR = 0.2, $p = 4x10^{-4}$, Figure 1, Supplemental Table 4), and the effect appears to be primarily co-dominant (p for trend = 0.001), as 47IV tended to be less protective than 47VV (though not significantly), and more protective than 47II (p = 0.04).

The protective effect of KIR3DL1 I47V is apparent considering alternative outcome measures

We next used a mixed linear effects model to estimate the effect of copy number of *KIR3DL1 47V* on longitudinally measured HIV VL and CD4 counts, adjusting for allelic effects of *HLA-A*, *-B*, *-C* and the time post-enrollment at which the VL was measured. The data were analyzed in all subjects combined, in those who

are *HLA-B Bw4+/B*57-*, and in *B*57* only subjects, where *KIR3DS1* and *KIR3DL1*004* were taken into account by being coded as random variables (Supplemental Table 1). Consistent with the above results, the strongest effect on longitudinal VL was seen in *B*57+* individuals where increasing copy number of *KIR3DL1 47V* was associated with significantly lower VL (-0.14 $\log_{10}$ copies/ml per *KIR3DL1 47V* allele, p = 4.9×10^{-18}; Table 2). The protective effect of *47V* was also observed when considering mVL (-0.18 $\log_{10}$ copies/ml per *KIR3DL1 47V* allele, p = 6.3×10^{-4}), and CD4+ T-cell counts, a marker of immunopathology due to HIV infection (increase of 24.88 cells/μl per *KIR3DL1 47V* allele, p = 1.5×10^{-6}; Table 2). In stark contrast, there was a significant detrimental effect of increasing copy number of *KIR3DL1 47V* among *Bw4+/B*57-* subjects, suggesting overt differential consequences attributable to the fine specificity of KIR/HLA allotypic interactions on natural killer (NK) cell function.

The effect of *KIR3DL1 I47V* variation on HIV control is specific to *B*57:01* and requires surface expressed *KIR3DL1* alleles

In an attempt to further explore the specificity of the *KIR3DL1 I47V/B*57* interaction, we next analyzed individual *B*57* subtypes. This analysis was restricted to *B*57:01* and *B*57:03,* because we had insufficient power to determine a reliable effect estimate for *B*57:02* and *B*57:04* (N = 28 and 3, respectively). Reminiscent of abacavir specifity for *B*57:01* (29-32), the protective effect of *KIR3DL1 I47V* on longitudinal VL was only observed among individuals with *B*57:01* (-0.36 $\log_{10}$ copies/ml, p = 1.7×10^{-67}; Table 3), with no

238 effect seen for *B*57:03* (0.01 $\log_{10}$ copies/ml, p = 0.16). Similar results were
239 observed for longitudinal CD4+ T-cell counts (90.9 cells/μl, p = $1.7x10^{-43}$ for
240 *B*57:01* vs. 20 cells/μl, p = 0.06 for *B*57:03*; Table 3), as well as for the
241 comparison of controllers vs. noncontrollers (*B*57:01* VV vs II: OR = 0.2, p =
242 0.001; *B*57:03* VV vs II: OR = 0.4, p = 0.25, data not shown).
243 We estimated the effect of each common *KIR3DL1* allele (see
244 Supplemental Table 3) on longitudinal viremia amongst *B*57*+ individuals in
245 order to compare association patterns between *B*57:01* vs. *B*57:03* as a
246 function of *KIR3DL1* subtype. The *47V* alleles *KIR3DL1*015* and **002*
247 associated with significantly lower VL levels, whereas the *47I* allele **001*
248 associated with higher VL amongst *B*57:01* subjects (Figure 2A). KIR3DL1*015
249 (2V/47V/54L) and KIR3DL1*001 (2M/47I/54I) have identical amino acid
250 sequences except for positions 2, 47, and 54 (Figure 2C), and it is therefore
251 notable that these two alleles modify *B*57:01* effects on HIV in opposite
252 directions. In *B*57:03*+ subjects, a distinct pattern of association was observed
253 where *KIR3DL1*002 (47V)* associated with high VL and **001* (*47I*) with protection
254 **(**Figure 2B**).** *KIR3DL1*004* (*47I* allele), which is not expressed at the cell surface
255 (25), showed no effect, consistent with the protective effect of *47V* being specific
256 to *KIR3DL1* (as opposed to it tagging variants in neighboring genes) and
257 requiring a surface expressed KIR3DL1 in conjunction with B*57:01. B*57:01 and
258 B*57:03 differ by only two amino acids, 114 (D vs. N, respectively) and 116 (S vs.
259 Y, respectively), which are located in the E and F pockets, respectively, of the
260 peptide binding groove, key pockets for determining which peptides will bind (30).

These data raise the possibility that presentation of peptide bound to B*57 molecules may determine, at least in part, whether 47V modulates protection conferred by the specific B*57 subtype or not.

The effect of KIR3DL1 I47V on ligand binding

Given the distal location of positions 2, 47 and 54 to the peptide-HLA binding interface (Supplemental Figure 3A), we hypothesized that these positons would not directly affect the binding affinity of the KIR3DL1 receptor on NK cells. Neverthelss, to better understand how polymorphisms at positions 2/47/54 impact recognition of the peptide-HLA-B*57:01 complex, we initially used surface plasmon resonance (SPR) to compare direct 1:1 binding of a number of B*57:01-peptide complexes to KIR3DL1*015 (2V/47V/54L) or KIR3DL1*001 and *005 (2M/47I/54I). In spite of the clear opposing effects of KIR3DL1*015 and KIR3DL1*001 on modifying B*57:01 protection (Figure 3A), these two KIR allotypes bound to B*57:01 with similar affinity, but with slightly weaker affinity than that to KIR3DL1*005. This confirmed that there was no strict correlation between 47V associated protection and higher affinity of 47V KIR3DL1 allotypes for B*57:01, at least with the peptides tested via SPR (Supplemental Figure 3B-E, Supplemental Table 5).

As differences in affinity were not observed in SPR, positions 2/47/54 might alter the avidity of KIR3DL1 through receptor clustering. Based on the crystal packing of the KIR3DL1-B*57:01 complex (33), a structural model of KIR3DL1 was constructed (Supplemental Figure 3A) where positions 47 and 54

are part of an extensive interface incorporating the α2 and α3 domains of neighboring HLA. This region is strictly conserved in B*57 allotypes and highly conserved across HLA alleles. In this model, each KIR3DL1 molecule thus makes contact with two HLA molecules to form higher order oligomers (i.e. clustering).

To further probe multimeric interactions between KIR3DL1-HLA, we assessed the binding of HLA-B*08:01 (negative control) and B*57:01 tetramers to 293T cells expressing FLAG-tagged KIR3DL1*001 or *015 (which differ only at positions 2, 47 and 54) or to mutant KIR3DL1 molecules containing reciprocal mutations at each position. Analyses of B*57 tetramer binding to cells expressing matched levels of KIR3DL1, as defined by equivalent staining with an anti-FLAG monoclonal antibody (mAb), showed increased binding to KIR3DL1*001 compared with *015 (Figure 3). Mutation of position 47 in the context of either KIR3DL1*001 or *015 had little impact on tetramer binding, whereas mutation of residue 54 resulted in an intermediate phenotype, subtly changing binding of B*57 tetramer to both KIR3DL1*001 and *015. In contrast, substitution of the M with V at position 2 of KIR3DL1*001 resulted in impaired binding, similar to that observed for KIR3DL1*015, but the reciprocal mutation in KIR3DL1*015 had no effect, suggesting its effect was dependent on the presence of 47I and/or 54I. Taken together, the data suggest that the dimorphisms at these three positions have little direct effect on affinity, consistent with their location distant to the ligand binding site of KIR3DL1 (Supplemental Figure 3A); yet in the context of multivalent binding, these residues may act coordinately in a manner that

307 impacts recognition of B*57, possibly affecting receptor clustering, thereby
308 affecting NK cell function.
309
310 **Discussion**
311 Superior HIV control amongst *B*57*+ subjects as a function of enhanced CTL
312 responses against B*57-restricted epitopes and the T cell receptors that
313 recognize the complex (12-14, 21, 34) cannot explain the sizeable heterogeneity
314 in HIV disease progression observed for *B*57*+ subjects. Analyses of our
315 European American seroconverter cohorts show that 50% of *B*57* positive
316 subjects have progressed to AIDS1993 (1993 definition of the US Center for
317 Disease Control) (35) by 11.2 years after infection, in comparison to 71% among
318 *B*57* negative subjects (data not shown). *B*57*+ controllers and non-controllers
319 present the same immunodominant B*57 restricted HIV gag epitopes and escape
320 mutations can occur in both groups (36). Thus, modifiers of B*57 responses
321 against HIV likely impact its efficacy.
322 We used a genome wide approach to interrogate genetic variants that
323 may enhance or diminish *B*57* protection among controllers vs. non-controllers,
324 and only a single variant encoding an isoleucine to valine change at position 47
325 in the KIR3DL1 molecule was identified. The association was conclusively
326 verified in a second cohort of viremic controllers compared to non-controllers ($p = 4 \times 10^{-3}$), and in an analysis of longitudinal VL and CD4 T cell counts ($p = 4.9 \times 10^{-18}$ and 1.5×10^{-6}, respectively), with each additional *3DL1 47V* as an additive
329 effect. Nevertheless, some *B*57:01*+ individuals with the protective *KIR3DL1 47V*

allele were noncontrollers, supporting a model in which a complex set of host and viral factors determine disease outcome among *B*57:01*+ subjects, *KIR3DL1 47V* being one of them. It is likely that variation in other regions of the genome that are difficult to decipher by GWAS, such as genes encoding T cell receptors, immunoglobulins and the leukocyte receptor complex (which includes the *KIR* genes), along with viral, environmental, and behavioral factors, are likely to impact the ability of *B*57*+ subjects to control HIV.

Stronger KIR3DL1-mediated inhibition of NK cells in the presence of HLA-B Bw4 subtypes that have isoleucine at position 80 (Bw4-80I) relative to those with threonine (Bw4-80T) (37) was the first indication of differential binding of KIR3DL1 to its various HLA-Bw4 ligands. Additional nuances in differential KIR3DL1/HLA-B interactions have since been reported, including recent studies suggesting variation in surface expression of both receptor and ligand (38) as well as differential binding capacity of specific KIR3DL1 allotypes to certain HLA-Bw4 ligands (24, 25, 38-40). High cell surface expression alleles of KIR3DL1 in combination with *HLA-B Bw4-80I* alleles, which includes *B*57*, were previously shown to be protective against HIV-1 (27). While there is overlap between 47V and high expression alleles (and between low expression alleles and 47I) (Supplemental Figure 2), the groupings are not identical. Most notably, KIR3DL1*001 is a high expression 47I allele and KIR3DL1*007 is a low expression 47V allele. The modifying effect of 47V appears to be B*57:01 specific, whereas the effect of high/low KIR3DL1 expression was observed for *HLA-B Bw4-80I* alleles overall. In light of our previous findings regarding

KIR3DL1 expression levels (27), as well as the protective effect of *KIR3DS1* in combination with *HLA-B Bw4-80I* (which includes *B*57*) (26), we performed a multivariate mixed linear effects analysis to determine the relative effects of *KIR3DL1 aa47*, KIR3DL1 expression level and *KIR3DS1* on HIV viremia in *B*57:01*+ and *B*57:03*+ subjects (see Supplemental Table 6). For *B*57:01*, the strongest and most significant *KIR3D* effect involves *KIR3DL1 47V* (effect estimate = -0.53 for each additional 47V copy; $p = 9 \times 10^{-86}$). Overall, the impact of KIR3DL1 variation on HIV outcome is multi-factorial and characterized by fine specificity between KIR3DL1 allotypes and their HLA-B+peptide ligands, which likely affects the NK cell response to HIV-infected cells.

Two common alleles containing 47V, *KIR3DL1*015* and **002*, each confer strong protection in combination with *B*57:01*, and these *KIR* alleles likely account in large part for the observed effect of 47V among *B*57:01*+ subjects (Figure 2). KIR3DL1*015 and *002 differ at only a single amino acid in the D2 domain, which is unlikely to alter the interaction with B*57:01. However, KIR3DL1*015 and *001, which differ only at amino acids 2, 47 and 54 (Figure 2C), convincingly show opposite modifying effects of *B*57:01*. This genetic epidemiological observation may be related to the reduction in binding of B*57:01 tetramers to KIR3DL1*015 relative to KIR3DL1*001 and *005 (41) (Figure 3). Perhaps HIV Nef downregulation of HLA-B in combination with reduced binding of KIR3DL1*015 to B*57:01 results in attenuated inhibitory signaling through this KIR, resulting in greater NK cell activation against HIV infected targets. Both HLA-B*57:01 and B*57:03 bind KIR3DL1 with high affinity as assessed by their

binding to bead-immobilized HLA class I allotypes. Indeed, HLA-B*57:01 has been the strongest KIR3DL1-binding HLA allotype irrespective of the KIR3DL1 allele tested, and B*57:03 has typically been in the top 10% of allotypes (40). As such, they would both be expected to license KIR3DL1+ NK cells quite well, but there is no data to address whether the small increment in KIR3DL1 binding shown in our study results in a difference in the number of licensed cells between B*57:01+ and B*57:03+ individuals.

In spite of differential tetramer binding to KIR3DL1*001 (47I) vs. *015 (47V), we did not detect clear differences in binding affinities of KIR3DL1*001 and *015 for B*57:01 by SPR (Supplemental Figure 3B-E; Supplemental Table 5). As these experiments were conducted with a limited number of peptides, any differences in affinity for B*57:01 conferred by positions 2, 47 and 54 may be apparent only across a diverse repertoire of peptides. It is also possible that positions 2, 47, and 54 may impact receptor clustering on NK cells and thus the avidity of the interaction. Differences in receptor clustering on the cell surface, a surrogate for signaling potential, may thereby alter the NK cell response to HIV infected targets. Positions 2, 47 and 54 also flank sites in D0 (positions 5, 31, and 32) that have been shown to be under positive natural selection (42), and there is data that further support the importance of these three positions in ligand binding (23).

Individually, the impact of mutations at positions 2, 47, or 54 of KIR3DL1 differed markedly, but each was dependent on the variants present at the other two positions (Figure 3), indicating that any potential effect of a given

399 polymorphism is dependent on the structural framework of the D0 domain.
400 Furthermore, mutagenesis experiments indicate that D0 is important for folding
401 and cell surface expression of KIR3DL1 (43) and contributes to binding avidity of
402 HLA ligand (44). Limited amino acid differences across KIR ligands can also
403 impact consequences of their interactions. B*57:01 and B*57:03 differ by two
404 amino acids (positions 114 and 116) in the peptide binding groove, and although
405 their peptide binding motifs are nearly indistinguishable, they do show some
406 differences in peptide preference (HIV Molecular Immunology Database:
407 hiv.lanl.gov), peptide positioning/presentation and immune pressure on the virus.
408 Crystal structures of HLA-B*57:01 and B*57:03 have been previously determined
409 by us and other groups (29, 30, 33, 45). Positions 114 (aspartate to asparagine)
410 and 116 (serine to tyrosine) lie in the floor of the peptide binding groove and
411 hence cannot directly contact KIR3DL1. Rather they alter the architecture and
412 charge of the E and F pockets. Thus, they likely impact the repertoire of peptides
413 that can bind each allotype and the way in which peptides are positioned in the
414 binding groove, thereby differentially altering the recognition of these peptide-
415 MHC complexes by any given KIR3DL1 subtype. Recent data also indicate that
416 KIR3DL1 polymorphisms contribute to differential binding preferences for HLA
417 class I allotypes, with B*57:01 showing better binding than B*57:03 (40). These
418 distinctions profoundly influence the modifying effects of specific *KIR3DL1* alleles
419 on the closely related *B*57:01* vs. *B*57:03* alleles (Figure 2), and emphasize the
420 granularity of KIR3DL1-HLA-B interactions.
421

MATERIALS and METHODS

Subjects

Data from a total of 3,878 HIV-1-infected individuals, including 818 *B*57*+ individuals (Whites = 482, Blacks = 270, other = 40, unknown = 26), were used in this study. The *B*57*+ individuals included 614 males (75.1%), 150 females (18.3%), 4 transgender (0.5%) and 50 individuals of unknown gender (6.1%). In the discovery phase, whole genome sequencing (WGS) was performed on 100 *B*57*+ HIV+ controllers (Whites = 90, other/unknown = 10) and 100 *B*57*+ HIV+ non-controllers (Whites = 97, other/unknown = 3). Controllers were antiretroviral therapy (ART) naïve individuals with at least 3 viral load (VL) measurements (most individuals had >6), the majority of which had <500 copies of HIV-1 RNA/ml of plasma (range = <500 - 1681, 89% <500), CD4+ T cell counts > 400/mm^3 and duration of infection > 4 years. Non-controllers included individuals with at least one VL > 10,000 copies/ml of plasma, and at least one CD4+ T cell count < 500/mm^3 (most had multiple CD4 counts < 500/mm^3).

Numbers for *B*57*+ individuals used in each outcome analysis are shown in Supplemental Table 1. For the mixed linear effects analysis, a total of 36,074 longitudinal viral load measurements were available for 3,865 individuals of all *HLA-B* genotypes (individuals with ≥1 viral load measurement), including 17,548 measurements for 674 *B*57*+ individuals. A total of 16,050 CD4 counts were available for 588 *B*57*+ individuals. There was an overlap of 566 *B*57*+ subjects between the categorical analyses (N = 710) and the mixed linear effects analyses (N = 674).

The subjects in this study were enrolled into one of eight cohorts: the Multicenter AIDS Cohort Study (MACS) (46), the AIDS linked to the Intravenous Experience (ALIVE) (47), the Massachusetts General Hospital controller cohort (MGH) (http://www.hivcontrollers.org/hivcontrollers), the Study on the Consequences of Protease Inhibitor Era (SCOPE) (48), the AIDS Clinical Trial Group cohort (ACTG) (https://actgnetwork.org), the Swiss HIV Cohort Study (SHCS) (http://www.shcs.ch), the U.S. military HIV Natural History Study (USMNHS) (www.idcrp.org), and the NIAID long term nonprogressor cohort (49). This study was approved by the protocol review office of the US National Cancer Institute institutional review board. Informed consent was obtained at the study sites from all individuals.

Whole genome sequencing (WGS).

Whole genome sequencing data was generated for 191/200 B*57+ samples on the Illumina HiSeq 2000 platform using 100bp paired-end reads. Samples were sequenced to an average depth of 36x coverage (range 29.9-53.4x). PCR duplicates were removed using picard-tools version 1.59 and unique reads were aligned to build 37 of the human genome reference sequencing using BWA version 0.5.10. Sequence variants were identified using GATK-1.6-11 and annotated using snpEff-3.3.

Two samples were found to have discordances between their self-declared gender and that inferred from the sequencing data using the estimated X:Y chromosome ratios and were excluded from further analysis. Two additional

samples were found to be duplicates based on 100% identity using a panel of 4000 common variants to test for cryptic relatedness between samples, and were also excluded. Thus, 187 samples were included in the genomewide analysis, of which 97 were controllers and 90 were non-controllers.

Associations between genetic variants and controller or noncontroller status were examined using both single variant tests and gene-based collapsing analyses of rare functional variants (minor allele frequency < 5%) using the ATAV software package (https://github.com/igm-team/atav). Significance scores were determined using Fisher's Exact test adjusted for multiple testing using a Bonferroni correction for the number of variants or genes included in each analysis.

***HLA* and *KIR* genotyping.** *HLA* genotyping was performed either by PCR-SSOP (sequence-specific oligonucleotide probing), PCR-SBT (sequence based typing) using the Sanger sequencing technology recommended by the 13th International Histocompatibility Workshop (http://www.ihwg.org), or next generation sequencing using the Roche 454 platform (50). *KIR* genotyping for presence/absence of *KIR* genes was performed by PCR-SSP (sequence specific priming) (51), followed by *KIR3DL1* sequencing using gene specific primers (52). Allele frequencies are shown in Supplemental Figure 2 and Supplemental Table 3. These frequencies are comparable to those seen in the general population (http://www.allelefrequencies.net/default.asp). *KIR3DL1* copy number was determined using a qualitative real-time PCR assay as previously described (28).

491 In cases where DNA was not available, copy number was imputed based on the
492 overall *KIR* profile and the results of *KIR3DL1* subtyping.
493
494 **Protein expression and purification**
495 The HLA-B*57:01 and β2-microglobulin genes were sub-cloned into the pET-30
496 expression vector and expressed separately into inclusion bodies in E. coli. The
497 HLA complex was refolded in the presence of the ISPRTLNAW (IW9, HIV-1 gag),
498 KAFSPEVIPMF (KF11, HIV-1 gag), QASQEVKNW (QW9, HIV-1 gag) and
499 LSSPVTKSF (LF9, self) peptides and purified as described previously (53).
500 KIR3DL1*001, *005 and *015 (residues 1 – 299) were sub-cloned into the
501 pFastBac insect expression vector with N-terminal 6xHis and secretion tags.
502 KIR3DL1 was expressed from Hi-5 insect cells (Invitrogen, Carlsbad, CA) and
503 secreted into the culture media. The protein was purified as described previously
504 (33) and then concentrated in a buffer comprised of 10 mM Tris pH 8.0, 300 mM
505 NaCl prior to use in surface plasmon resonance experiments.
506
507 **Surface Plasmon Resonance**
508 Surface plasmon resonance experiments (SPR) were used to measure the
509 affinities of KIR3DL1*001, *005 and *015 to HLA-B*57:01 presenting the HIV-1
510 gag epitopes IW9, KF11 and QW9 and the self-epitope LF9. SPR experiments
511 were conducted on a Biacore 3000 instrument at 298 K. A CM5 chip was used to
512 immobilize the anti-HLA monoclonal antibody W6/32 (generated in house (54))
513 via amine coupling. HLA-B*57:01-peptide complexes were then captured on the

chip by binding to W6/32 to a surface density of ~ 700 response units. KIR3DL1*001 (2.25–350 μM), *005 (2.25–350 μM) and *015 (1.56 to 200 μM) were injected over the chip at a flow rate of 5 μL/min in a buffer comprised of 10 mM HEPES-HCl pH 7.4, 150 mM NaCl and 0.005% surfactant P20. The response to the W6/32 alone control flow cell was subtracted from the responses to HLA-B*57:01-peptides. Equilibrium data were analysed using GraphPad Prism. All data are representative of two independent experiments, with each experiment conducted with duplicate samples. Error bars represent standard error.

Tetramer Binding Assay

pEF6.FLAG-tagged KIR3DL1*001 and *015 constructs (41) were mutated at residues 2, 47 and 54 via site directed mutagenesis. pEF6.KIR3DL1*001/*015 were transfected into 293T cells using FuGENE 6 transfection reagent (Promega, Madison, WI) according to the manufacturer's instructions and KIR3DL1 surface expression was confirmed via staining with NKB1-FITC (clone DX9, BD Pharmingen, San Jose, CA) after 48 hours. Transfected 293T cells (originally purchased from ATCC) were stained with 350ng/test tetrameric HLA-B*57:01/LF9 or HLA-B*08:01/FLR conjugated with PE-SA and incubated at room temperature for 30 minutes. Cells were washed and stained with anti-FLAG-APC (clone L5, BioLegend, San Diego, CA) before analysis by flow cytometry.

Statistical analyses

SAS 9.2 (SAS Institute) or *R* 3.3.1 (The R Foundation) was used for data management and statistical analyses. PROC FREQ was used to compute frequencies on categorical variables. PROC LOGISTIC was used to calculate odds ratios and 95% confidence intervals. These analyses were performed with combined Whites, Blacks and other races (Hispanic/Latino, Asian) adjusting for race. Statistical significance refers to two-sided P values of <0.05.

Analyses of the longitudinal viral load and CD4+ T-cell count were performed using the *lmer* function in R. We allowed for random effects due to each *HLA-A*, *-B* and *-C* allele (or where modified, as specified in the results section), the time post enrolment and a correction for diploid *HLA* allele coding. Several alternative outcomes were tested, including the $\log_{10}$ transformed HIV viral load (VL) at each timepoint, a geometric mean HIV VL (mVL) of all timepoints and the CD4+ T-cell count at each timepoint. Likelihood ratio p values were calculated using the ANOVA function in R in order to compare nested models fit under a maximum-likelihood scenario. The p values reported are not adjusted for multiple comparisons.

Study Approval

This study was reviewed and approved by the protocol review office of the US National Cancer Institute Office of Human Subjects Research Protections (OHSRP), The Warren Magnuson Clinical Center (Building 10), Room 2C146,

Bethesda, MD 20892. Informed consent was obtained at the study sites from all individuals prior to their participation in the study.

Author Contributions

M.C. designed the study; M.C., M.P.M., V.N. wrote the manuscript; M.P.M, P.S., V.R., X.G., P.P., P.M.S., J.W., S.C.W., D.P., B.L. contributed to experiments; V.N., Y.Q., N.V., J.P.V., J.R., A.G.B., Z.B., J.M.C. contributed to data analyses; R.T. coordinated sample selection for WGS; S.W., J.J.G., B.W., F.P., S.D., D.W.H., S.M., M.C., N.M., J.F. contributed study cohort samples; M.C., V.N., M.P.M., J.R., J.P.V., A.G.B. contributed to data interpretation. All authors contributed to manuscript revision.

Acknowledgements

This article is dedicated to the memory of Dr. Bonnie Mathieson, a longtime friend and colleague who dedicated her career to the advancement of HIV research. We would like to thank Victoria Walker-Sperling for her generous assistance with figures. This work was supported by federal funds from the National Cancer Institute, National Institutes of Health (NIH) under contract HHSN261200800001E. The content of this publication does not necessarily reflect the views or policies of the Departments of the Army and Defense or Health and Human Services, nor does mention of trade names, commercial products, or organizations imply endorsement by the US Government. This Research was supported in part by the Intramural Research Program of the NIH,

583 Frederick National Lab, Center for Cancer Research and the National Health and
584 Medical Research Council, Australia.

585 Data in this manuscript were collected by the Multicenter AIDS Cohort
586 Study (MACS) and/or the Women's Interagency HIV Study (WIHS). The
587 contents of this publication are solely the responsibility of the authors and do not
588 represent the official views of the National Institutes of Health (NIH). MACS
589 (Principal Investigators): Johns Hopkins University Bloomberg School of Public
590 Health (Joseph Margolick), U01-AI35042; Northwestern University (Steven
591 Wolinsky), U01-AI35039; University of California, Los Angeles (Roger Detels),
592 U01-AI35040; University of Pittsburgh (Charles Rinaldo), U01-AI35041; the
593 Center for Analysis and Management of MACS, Johns Hopkins University
594 Bloomberg School of Public Health (Lisa Jacobson), UM1-AI35043. The MACS is
595 funded primarily by the National Institute of Allergy and Infectious Diseases
596 (NIAID), with additional co-funding from the National Cancer Institute (NCI).
597 Targeted supplemental funding for specific projects was also provided by the
598 National Heart, Lung, and Blood Institute (NHLBI), and the National Institute on
599 Deafness and Communication Disorders (NIDCD). MACS data collection is also
600 supported by UL1-TR000424 (JHU CTSA). Website located at
601 www.statepi.jhsph.edu/macs/macs.html.

602 The AIDS Clinical Trials Group (ACTG) was supported by NIH grants
603 AI068636, AI038858, AI068634, AI038855, and grants to sites AI069513,
604 AI34835, AI069432, AI069423, AI069477, AI069501, AI069474, AI069428,
605 AI69467, AI069415, AI32782, AI27661, AI25859, AI28568, AI30914, AI069495,

606 AI069471, AI069532, AI069452, AI069450, AI069556, AI069484, AI069472,
607 AI34853, AI069465, AI069511, AI38844, AI069424, AI069434, AI46370,
608 AI069502, AI069419, and RR024975. David Haas is also supported by NIH
609 grants AI077505, AI110527 and TR000445.
610 J.R. is supported by the National Health and Medical Research Council of
611 Australia, the Anti-cancer council, Australian Research Council, and an ARC
612 Laureate Fellowship. Z.L.B. is supported by a Scholar Award from the Michael
613 Smith Foundation for Health Research. D.A.P. Is a Wellcome Trust Senior
614 Investigator.
615

References

1. Carrington M, and O'Brien SJ. The influence of HLA genotype on AIDS. *Annu Rev Med.* 2003;54(535-51.
2. Fellay J, Shianna KV, Ge D, Colombo S, Ledergerber B, Weale M, Zhang K, Gumbs C, Castagna A, Cossarizza A, et al. A whole-genome association study of major determinants for host control of HIV-1. *Science.* 2007;317(5840):944-7.
3. Pereyra F, Jia X, McLaren PJ, Telenti A, de Bakker PI, Walker BD, Ripke S, Brumme CJ, Pulit SL, Carrington M, et al. The major genetic determinants of HIV-1 control affect HLA class I peptide presentation. *Science.* 2010;330(6010):1551-7.
4. Gao X, Bashirova A, Iversen AK, Phair J, Goedert JJ, Buchbinder S, Hoots K, Vlahov D, Altfeld M, O'Brien SJ, et al. AIDS restriction HLA allotypes target distinct intervals of HIV-1 pathogenesis. *Nature Med.* 2005;11(12):1290-2.
5. Kaslow RA, Carrington M, Apple R, Park L, Munoz A, Saah AJ, Goedert JJ, Winkler C, O'Brien SJ, Rinaldo C, et al. Influence of combinations of human major histocompatibility complex genes on the course of HIV-1 infection. *Nat Med.* 1996;2(4):405-11.
6. Kiepiela P, Leslie AJ, Honeyborne I, Ramduth D, Thobakgale C, Chetty S, Rathnavalu P, Moore C, Pfafferott KJ, Hilton L, et al. Dominant influence of HLA-B in mediating the potential co-evolution of HIV and HLA. *Nature.* 2004;432(7018):769-75.
7. Magierowska M, Theodorou I, Debre P, Sanson F, Autran B, Riviere Y, Charron D, and Costagliola D. Combined genotypes of CCR5, CCR2, SDF1, and HLA genes can predict the long-term nonprogressor status in human immunodeficiency virus-1- infected individuals. *Blood.* 1999;93(3):936-41.
8. Migueles SA, Sabbaghian MS, Shupert WL, Bettinotti MP, Marincola FM, Martino L, Hallahan CW, Selig SM, Schwartz D, Sullivan J, et al. HLA B*5701 is highly associated with restriction of virus replication in a subgroup of HIV-infected long term nonprogressors. *Proc Natl Acad Sci U S A.* 2000;97(6):2709-14.
9. Gao X, Nelson GW, Karacki P, Martin MP, Phair J, Kaslow R, Goedert JJ, Buchbinder S, Hoots K, Vlahov D, et al. Effect of a single amino acid change in MHC class I molecules on the rate of progression to AIDS. *N Engl J Med.* 2001;344(22):1668-75.
10. Deeks SG, and Walker BD. Human immunodeficiency virus controllers: mechanisms of durable virus control in the absence of antiretroviral therapy. *Immunity.* 2007;27(3):406-16.
11. Emu B, Sinclair E, Hatano H, Ferre A, Shacklett B, Martin JN, McCune JM, and Deeks SG. HLA class I-restricted T-cell responses may contribute to the control of human immunodeficiency virus infection, but such responses are not always necessary for long-term virus control. *J Virol.* 2008;82(11):5398-407.

12. Gillespie GM, Kaul R, Dong T, Yang HB, Rostron T, Bwayo JJ, Kiama P, Peto T, Plummer FA, McMichael AJ, et al. Cross-reactive cytotoxic T lymphocytes against a HIV-1 p24 epitope in slow progressors with B*57. *Aids.* 2002;16(7):961-72.
13. Goulder PJ, Bunce M, Krausa P, McIntyre K, Crowley S, Morgan B, Edwards A, Giangrande P, Phillips RE, and McMichael AJ. Novel, cross-restricted, conserved, and immunodominant cytotoxic T lymphocyte epitopes in slow progressors in HIV type 1 infection. *AIDS Res Hum Retroviruses.* 1996;12(18):1691-8.
14. Kiepiela P, Ngumbela K, Thobakgale C, Ramduth D, Honeyborne I, Moodley E, Reddy S, de Pierres C, Mncube Z, Mkhwanazi N, et al. CD8+ T-cell responses to different HIV proteins have discordant associations with viral load. *Nat Med.* 2007;13(1):46-53.
15. Brockman MA, Schneidewind A, Lahaie M, Schmidt A, Miura T, Desouza I, Ryvkin F, Derdeyn CA, Allen S, Hunter E, et al. Escape and compensation from early HLA-B57-mediated cytotoxic T-lymphocyte pressure on human immunodeficiency virus type 1 Gag alter capsid interactions with cyclophilin A. *J Virol.* 2007;81(22):12608-18.
16. Crawford H, Lumm W, Leslie A, Schaefer M, Boeras D, Prado JG, Tang J, Farmer P, Ndung'u T, Lakhi S, et al. Evolution of HLA-B*5703 HIV-1 escape mutations in HLA-B*5703-positive individuals and their transmission recipients. *The Journal of experimental medicine.* 2009;206(4):909-21.
17. Leslie AJ, Pfafferott KJ, Chetty P, Draenert R, Addo MM, Feeney M, Tang Y, Holmes EC, Allen T, Prado JG, et al. HIV evolution: CTL escape mutation and reversion after transmission. *Nat Med.* 2004;10(3):282-9.
18. Martinez-Picado J, Prado JG, Fry EE, Pfafferott K, Leslie A, Chetty S, Thobakgale C, Honeyborne I, Crawford H, Matthews P, et al. Fitness cost of escape mutations in p24 Gag in association with control of human immunodeficiency virus type 1. *J Virol.* 2006;80(7):3617-23.
19. Miura T, Brockman MA, Schneidewind A, Lobritz M, Pereyra F, Rathod A, Block BL, Brumme ZL, Brumme CJ, Baker B, et al. HLA-B57/B*5801 human immunodeficiency virus type 1 elite controllers select for rare gag variants associated with reduced viral replication capacity and strong cytotoxic T-lymphocyte [corrected] recognition. *Journal of virology.* 2009;83(6):2743-55.
20. Carlson JM, Du VY, Pfeifer N, Bansal A, Tan VY, Power K, Brumme CJ, Kreimer A, DeZiel CE, Fusi N, et al. Impact of pre-adapted HIV transmission. *Nat Med.* 2016;22(6):606-13.
21. Turnbull EL, Lopes AR, Jones NA, Cornforth D, Newton P, Aldam D, Pellegrino P, Turner J, Williams I, Wilson CM, et al. HIV-1 epitope-specific CD8+ T cell responses strongly associated with delayed disease progression cross-recognize epitope variants efficiently. *J Immunol.* 2006;176(10):6130-46.
22. Kosmrlj A, Read EL, Qi Y, Allen TM, Altfeld M, Deeks SG, Pereyra F, Carrington M, Walker BD, and Chakraborty AK. Effects of thymic selection

of the T-cell repertoire on HLA class I-associated control of HIV infection. *Nature.* 2010;465(7296):350-4.
23. Sharma D, Bastard K, Guethlein LA, Norman PJ, Yawata N, Yawata M, Pando M, Thananchai H, Dong T, Rowland-Jones S, et al. Dimorphic motifs in D0 and D1+D2 domains of killer cell Ig-like receptor 3DL1 combine to form receptors with high, moderate, and no avidity for the complex of a peptide derived from HIV and HLA-A*2402. *J Immunol.* 2009;183(7):4569-82.
24. Gardiner CM, Guethlein LA, Shilling HG, Pando M, Carr WH, Rajalingam R, Vilches C, and Parham P. Different NK cell surface phenotypes defined by the DX9 antibody are due to KIR3DL1 gene polymorphism. *J Immunol.* 2001;166(5):2992-3001.
25. Pando MJ, Gardiner CM, Gleimer M, McQueen KL, and Parham P. The protein made from a common allele of KIR3DL1 (3DL1*004) is poorly expressed at cell surfaces due to substitution at positions 86 in Ig domain 0 and 182 in Ig domain 1. *J Immunol.* 2003;171(12):6640-9.
26. Martin MP, Gao X, Lee JH, Nelson GW, Detels R, Goedert JJ, Buchbinder S, Hoots K, Vlahov D, Trowsdale J, et al. Epistatic interaction between KIR3DS1 and HLA-B delays the progression to AIDS. *Nature Genet.* 2002;31(4):429-34.
27. Martin MP, Qi Y, Gao X, Yamada E, Martin JN, Pereyra F, Colombo S, Brown EE, Shupert WL, Phair J, et al. Innate partnership of HLA-B and KIR3DL1 subtypes against HIV-1. *Nat Genet.* 2007;39(6):733-40.
28. Pelak K, Need AC, Fellay J, Shianna KV, Feng S, Urban TJ, Ge D, De Luca A, Martinez-Picado J, Wolinsky SM, et al. Copy number variation of KIR genes influences HIV-1 control. *PLoS biology.* 2011;9(11):e1001208.
29. Chessman D, Kostenko L, Lethborg T, Purcell AW, Williamson NA, Chen Z, Kjer-Nielsen L, Mifsud NA, Tait BD, Holdsworth R, et al. Human leukocyte antigen class I-restricted activation of CD8+ T cells provides the immunogenetic basis of a systemic drug hypersensitivity. *Immunity.* 2008;28(6):822-32.
30. Illing PT, Vivian JP, Dudek NL, Kostenko L, Chen Z, Bharadwaj M, Miles JJ, Kjer-Nielsen L, Gras S, Williamson NA, et al. Immune self-reactivity triggered by drug-modified HLA-peptide repertoire. *Nature.* 2012;486(7404):554-8.
31. Mallal S, Nolan D, Witt C, Masel G, Martin AM, Moore C, Sayer D, Castley A, Mamotte C, Maxwell D, et al. Association between presence of HLA-B*5701, HLA-DR7, and HLA-DQ3 and hypersensitivity to HIV-1 reverse-transcriptase inhibitor abacavir. *Lancet.* 2002;359(9308):727-32.
32. Norcross MA, Luo S, Lu L, Boyne MT, Gomarteli M, Rennels AD, Woodcock J, Margulies DH, McMurtrey C, Vernon S, et al. Abacavir induces loading of novel self-peptides into HLA-B*57: 01: an autoimmune model for HLA-associated drug hypersensitivity. *AIDS.* 2012;26(11):F21-9.
33. Vivian JP, Duncan RC, Berry R, O'Connor GM, Reid HH, Beddoe T, Gras S, Saunders PM, Olshina MA, Widjaja JM, et al. Killer cell

immunoglobulin-like receptor 3DL1-mediated recognition of human leukocyte antigen B. *Nature.* 2011;479(7373):401-5.
34. Chen H, Ndhlovu ZM, Liu D, Porter LC, Fang JW, Darko S, Brockman MA, Miura T, Brumme ZL, Schneidewind A, et al. TCR clonotypes modulate the protective effect of HLA class I molecules in HIV-1 infection. *Nat Immunol.* 2012;13(7):691-700.
35. 1993 revised classification system for HIV infection and expanded surveillance case definition for AIDS among adolescents and adults. *MMWR Morb Mortal Wkly Rep.* 1992;41(RR-17):1-19.
36. Migueles SA, Laborico AC, Imamichi H, Shupert WL, Royce C, McLaughlin M, Ehler L, Metcalf J, Liu S, Hallahan CW, et al. The differential ability of HLA B*5701+ long-term nonprogressors and progressors to restrict human immunodeficiency virus replication is not caused by loss of recognition of autologous viral gag sequences. *Journal of virology.* 2003;77(12):6889-98.
37. Cella M, Longo A, Ferrara GB, Strominger JL, and Colonna M. NK3-specific natural killer cells are selectively inhibited by Bw4- positive HLA alleles with isoleucine 80. *J Exp Med.* 1994;180(4):1235-42.
38. Boudreau JE, Mulrooney TJ, Le Luduec JB, Barker E, and Hsu KC. KIR3DL1 and HLA-B Density and Binding Calibrate NK Education and Response to HIV. *J Immunol.* 2016;196(8):3398-410.
39. Gumperz JE, Barber LD, Valiante NM, Percival L, Phillips JH, Lanier LL, and Parham P. Conserved and variable residues within the Bw4 motif of HLA-B make separable contributions to recognition by the NKB1 killer cell-inhibitory receptor. *J Immunol.* 1997;158(11):5237-41.
40. Saunders PM, Pymm P, Pietra G, Hughes VA, Hitchen C, O'Connor GM, Loiacono F, Widjaja J, Price DA, Falco M, et al. Killer cell immunoglobulin-like receptor 3DL1 polymorphism defines distinct hierarchies of HLA class I recognition. *J Exp Med.* 2016;213(5):791-807.
41. O'Connor GM, Vivian JP, Widjaja JM, Bridgeman JS, Gostick E, Lafont BA, Anderson SK, Price DA, Brooks AG, Rossjohn J, et al. Mutational and structural analysis of KIR3DL1 reveals a lineage-defining allotypic dimorphism that impacts both HLA and peptide sensitivity. *J Immunol.* 2014;192(6):2875-84.
42. Norman PJ, Abi-Rached L, Gendzekhadze K, Korbel D, Gleimer M, Rowley D, Bruno D, Carrington CV, Chandanayingyong D, Chang YH, et al. Unusual selection on the KIR3DL1/S1 natural killer cell receptor in Africans. *Nature Genet.* 2007;39(9):1092-9.
43. Rojo S, Wagtmann N, and Long EO. Binding of a soluble p70 killer cell inhibitory receptor to HLA-B*5101: requirement for all three p70 immunoglobulin domains. *Eur J Immunol.* 1997;27(2):568-71.
44. Khakoo SI, Geller R, Shin S, Jenkins JA, and Parham P. The D0 domain of KIR3D acts as a major histocompatibility complex class I binding enhancer. *J Exp Med.* 2002;196(7):911-21.
45. Stewart-Jones GB, Gillespie G, Overton IM, Kaul R, Roche P, McMichael AJ, Rowland-Jones S, and Jones EY. Structures of three HIV-1 HLA-

B*5703-peptide complexes and identification of related HLAs potentially associated with long-term nonprogression. *J Immunol.* 2005;175(4):2459-68.

46. Phair J, Jacobson L, Detels R, Rinaldo C, Saah A, Schrager L, and Munoz A. Acquired immune deficiency syndrome occurring within 5 years of infection with human immunodeficiency virus type-1: the Multicenter AIDS Cohort Study. *J Acquir Immune Defic Syndr.* 1992;5(5):490-6.
47. Vlahov D, Anthony JC, Munoz A, Margolick J, Nelson KE, Celentano DD, Solomon L, and Polk BF. The ALIVE study, a longitudinal study of HIV-1 infection in intravenous drug users: description of methods and characteristics of participants. *NIDA Res Monogr.* 1991;109(75-100.
48. Emu B, Sinclair E, Favre D, Moretto WJ, Hsue P, Hoh R, Martin JN, Nixon DF, McCune JM, and Deeks SG. Phenotypic, functional, and kinetic parameters associated with apparent T-cell control of human immunodeficiency virus replication in individuals with and without antiretroviral treatment. *J Virol.* 2005;79(22):14169-78.
49. Migueles SA, Laborico AC, Shupert WL, Sabbaghian MS, Rabin R, Hallahan CW, Van Baarle D, Kostense S, Miedema F, McLaughlin M, et al. HIV-specific CD8+ T cell proliferation is coupled to perforin expression and is maintained in nonprogressors. *Nat Immunol.* 2002;3(11):1061-8.
50. Holcomb CL, Hoglund B, Anderson MW, Blake LA, Bohme I, Egholm M, Ferriola D, Gabriel C, Gelber SE, Goodridge D, et al. A multi-site study using high-resolution HLA genotyping by next generation sequencing. *Tissue Antigens.* 2011;77(3):206-17.
51. Martin MP, and Carrington M. KIR locus polymorphisms: genotyping and disease association analysis. *Methods Mol Biol.* 2008;415(49-64.
52. Thomas R, Yamada E, Alter G, Martin MP, Bashirova AA, Norman PJ, Altfeld M, Parham P, Anderson SK, McVicar DW, et al. Novel KIR3DL1 alleles and their expression levels on NK cells: convergent evolution of KIR3DL1 phenotype variation? *J Immunol.* 2008;180(10):6743-50.
53. Clements CS, Kjer-Nielsen L, MacDonald WA, Brooks AG, Purcell AW, McCluskey J, and Rossjohn J. The production, purification and crystallization of a soluble heterodimeric form of a highly selected T-cell receptor in its unliganded and liganded state. *Acta Crystallogr D Biol Crystallogr.* 2002;58(Pt 12):2131-4.
54. Barnstable CJ, Bodmer WF, Brown G, Galfre G, Milstein C, Williams AF, and Ziegler A. Production of monoclonal antibodies to group A erythrocytes, HLA and other human cell surface antigens-new tools for genetic analysis. *Cell.* 1978;14(1):9-20.

Figure Legends

Figure 1: Influence of KIR3DL1 amino acid 47 on HIV control in *HLA-B*57+* individuals. Only individuals with two expressed KIR3DL1 alleles were included in the analysis. Individuals with *KIR3DS1, KIR3DL1*004* (1 or 2 copies) and *KIR3DL1+/-* (i.e. *KIR3DL1/S1* missing on one haplotype) were excluded. Statistical analysis was performed using logistic regression. CTR = HIV controllers (N = 188); NC = non-controllers (N = 136). OR = odds ratio. *Numbers above the bars refer to the number of individuals in each group.

Figure 2: Effect of individual *KIR3DL1* alleles on longitudinal HIV viremia in subjects with *B*57* subtypes. We used a mixed linear effects model adjusting for all *HLA-A, -B* and *-C* alleles and time post enrolment to estimate the effect of each *KIR3DL1* allele for groups including individuals with (a) *B*57:01* only, (b) *B*57:03* only. 47I alleles are shown in red and 47V alleles are shown in blue. Bars represent 95% confidence interval. The size of the black dots is scaled by the frequency of each allele. Alleles with estimates that do not cross the line, which represents no change in VL (0), are significant. c) Extracellular domain amino acid alignment of the KIR3DL1 alleles tested in A and B (http://www.ebi.ac.uk/ipd/kir/). Red = D0, green = D1, blue = D2. Positions 2, 47 and 54 are highlighted in yellow.

Figure 3: HLA-B*57:01/LF9 tetramer binding to KIR3DL1 variants. 293T cells were transfected with FLAG-tagged KIR3DL1*001, *015 or mutants and stained

with HLA-B*57:01/LF9 or HLA-B*08:01/FLR tetramers (350ng each). a) The MFI of HLA-B*57:01/LF9 binding to FLAG-positive sections from a representative experiment (in triplicate) is depicted, where statistical significance was assessed by ANOVA with a Tukey multiple comparison test. Error bars represent SE of the mean. ****$p < 0.0001$. b) The MFI of tetramer staining on FLAG-positive sections is normalized to HLA-B*57:01/LF9 binding to KIR3DL1*001 across four independent transfection experiments. Error bars represent SE of the mean.

Table 1: Allele frequency of *rs643347*G/A in two independent *B*57+* cohorts[A]

	WGS N = 159[B]			Validation N = 510		
***rs643347* allele**	**CTR N (%)**	**NC N (%)**	**P value**	**CTR N (%)**	**NC N (%)**	**P value**
G	73 (43.5)	25 (16.7)	2.4×10^{-7}	338 (56.9)	203 (47.7)	0.004
A	95 (56.5)	125 (83.3)		256 (43.1)	223 (52.3)	

CTR = controllers; NC = non-controllers

[A]Single variant analysis using Fisher's exact test

[B]High quality sequence data for I47V was available for 159 of the 187 samples that were included in the genomewide analysis.

Table 2: Effect of *KIR3DL1 I47V* on various outcomes[A]

	Outcome Measure	N II/IV/VV	Effect[B] (linear estimate)	SE	p value
All	Longitudinal log_{10}VL	3865 1309/1800/756	0.003	0.008	0.69
HLA-B Bw4+/B*57-	Longitudinal log_{10}VL	2022 659/958/405	0.09	0.012	2.2×10^{-13}
B*57+	Longitudinal log_{10}VL	674 238/306/130	-0.14	0.016	4.9×10^{-18}
B*57+	Mean Viral Load (mVL)	674 238/306/130	-0.18	0.05	6.3×10^{-4}
B*57+	Longitudinal CD4 count	588 208/272/108	24.88	4.13	1.5×10^{-6}

[A]*HLA-A, -B* and *-C* alleles, timing of viral loads measurements as well as presence of *KIR3DL1*004* and *KIR3DS1* were taken into account by being coded as random effects for all analyses using a mixed linear effects model.

[B]Effect estimates denote the effect of each additional *3DL1 47V* as an additive effect.

Table 3: Effect of KIR3DL1 I47V on logVL and CD4+ T-cell counts in individuals with *B*57:01* and *B*57:03*[A]

Genotype	N	Outcome	Effect[B] (linear estimate)	SE	p value
B*57:01+	398	Longitudinal log_{10}VL	-0.36	0.02	1.7×10^{-67}
B*57:03+	245		0.01	0.03	0.16
B*57:01+	383	Longitudinal CD4 count	90.9	6.53	4.8×10^{-43}
B*57:03+	241		20	9.4	0.06

[A]*HLA-A, -B* and *-C* alleles, timing of viral loads measurements as well as presence of *KIR3DL1*004* and *KIR3DS1* were taken into account by being coded as random effects for all analyses using a mixed linear effects model.
[B]Effect estimates denote the effect of each additional 3DL1 47V as an additive effect.

Figure 1

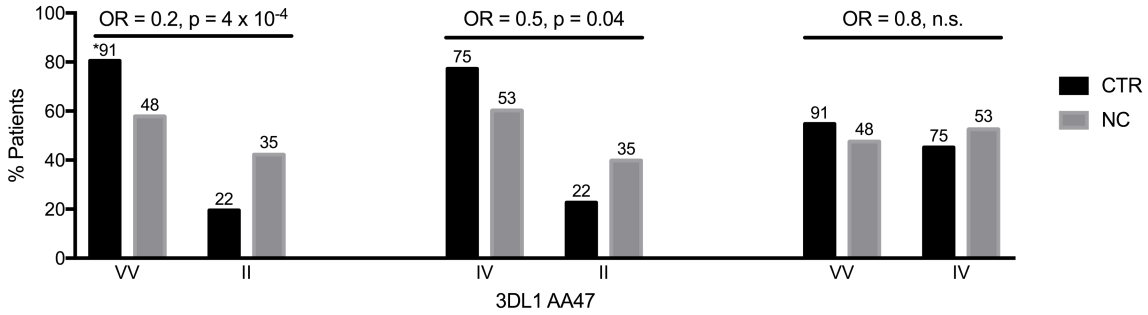

Figure 1: Influence of KIR3DL1 amino acid 47 on HIV control in *HLA-B*57*+ individuals. Only individuals with two expressed KIR3DL1 alleles were included in the analysis. Individuals with *KIR3DS1, KIR3DL1*004* (1 or 2 copies) and *KIR3DL1*+/- (i.e. *KIR3DL1/S1* missing on one haplotype) were excluded. Statistical analysis was performed using logistic regression. CTR = HIV controllers (N = 188); NC = non-controllers (N = 136). OR = odds ratio. *Numbers above the bars refer to the number of individuals in each group.

Figure 2

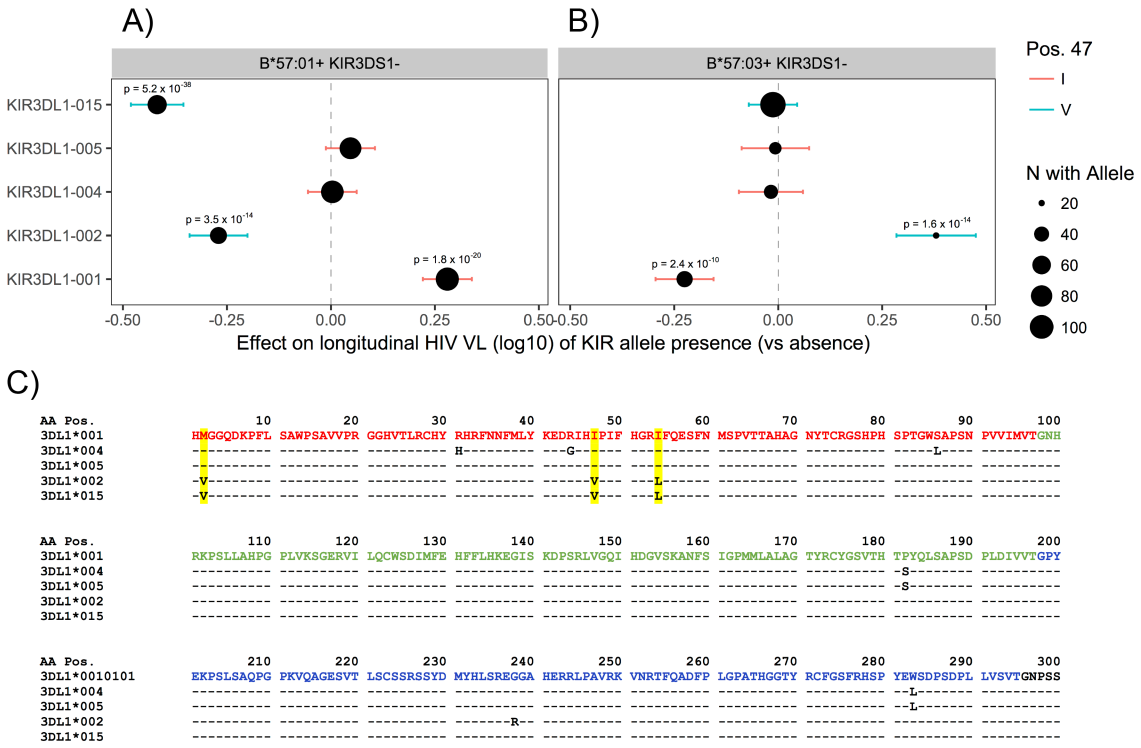

Figure 2: Effect of individual *KIR3DL1* alleles on longitudinal HIV viremia in subjects with *B*57* subtypes. We used a mixed linear effects model adjusting for all *HLA-A, -B* and *-C* alleles and time post enrolment to estimate the effect of each *KIR3DL1* allele for groups including individuals with (a) *B*57:01* only, (b) *B*57:03* only. 47I alleles are shown in red and 47V alleles are shown in blue. Bars represent 95% confidence interval. The size of the black dots is scaled by the frequency of each allele. Alleles with estimates that do not cross the line, which represents no change in VL (0), are significant. c) Extracellular domain amino acid alignment of the KIR3DL1 alleles tested in A and B (http://www.ebi.ac.uk/ipd/kir/). Red = D0, green = D1, blue = D2. Positions 2, 47 and 54 are highlighted in yellow.

917

Figure 3

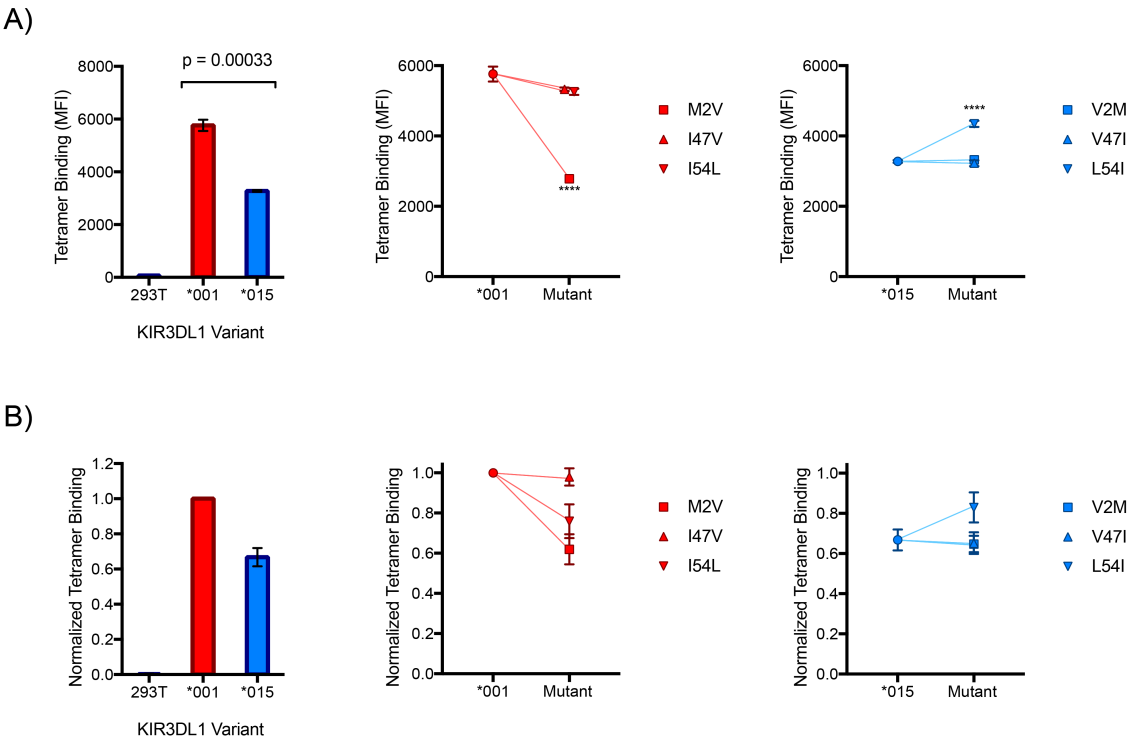

Figure 3: HLA-B*57:01/LF9 tetramer binding to KIR3DL1 variants. 293T cells were transfected with FLAG-tagged KIR3DL1*001, *015 or mutants and stained with HLA-B*57:01/LF9 or HLA-B*08:01/FLR tetramers (350ng each). a) The MFI of HLA-B*57:01/LF9 binding to FLAG-positive sections from a representative experiment (in triplicate) is depicted, where statistical significance was assessed by ANOVA with a Tukey multiple comparison test. Error bars represent SE of the mean. ****$p < 0.0001$. b) The MFI of tetramer staining on FLAG-positive sections is normalized to HLA-B*57:01/LF9 binding to KIR3DL1*001 across four independent transfection experiments. Error bars represent SE of the mean.

Supplemental Table 1: Characteristics of the *B*57+* study population

Outcome measure	Controllers	Noncontrollers
Whole Genome Sequencing Single variant analysis	**N = 100** W=90, other=10	**N = 100** W=97, other=3
Single variant analysis (validation cohort)	**N = 297** W=136, B=139, other=22	**N = 213** W=115, B=91, other=7
Genotypic analysis	**N = 188** W=80, B=92, other=16	**N = 136** W=72, B=59, other=5
Longitudinal log_{10}VL	**N = 674** W=389, B=221, other=64	
Mean viral load (mVL)	**N = 674** W=389, B=221, other=64	
Longitudinal CD4 count	**N = 588** W=338, B=194, other=56	

W = Whites; B = Blacks; Other = Hispanic/Latino, Asian, mixed race, unknown race.

Supplemental Table 2: Pairwise LD analysis of KIR3DL1 amino acids 2,47 and 54

	Caucasians		African Americans	
	aa47	**aa54**	**aa47**	**aa54**
aa2				
r^2	0.92	0.99	0.69	0.74
D'	1.00	1.00	1.00	1.00
aa47				
r^2		0.93		0.93
D'		1.00		1.00

Supplemental Table 3: KIR3DL1 allele frequencies in controllers and noncontrollers[A]

	Whites		Blacks	
3DL1 allele	**CTR N (%)**	**NC N (%)**	**CTR N (%)**	**NC N (%)**
001	78 (15.4)	79 (20.0)	33 (11.3)	15 (8.5)
002	62 (12.3)	29 (7.4)	9 (3.1)	8 (4.5)
004	77 (15.2)	73 (18.5)	27 (9.2)	15 (8.5)
005	71 (14.1)	72 (18.3)	16 (5.1)	10 (5.7)
007	12 (2.4)	5 (1.3)	12 (4.1)	9 (5.1)
008	23 (4.6)	25 (6.3)	3 (1.0)	1 (0.6)
009	10 (2.0)	3 (0.8)	5 (1.7)	0 (0)
015/017	55 (10.9)	22 (5.6)	123 (42.0)	72 (40.9)
020	12 (2.4)	3 (0.8)	16 (5.5)	11 (6.2)
3DS1[B]	100 (19.8)	72 (18.3)	16 (5.5)	10 (5.7)

[A]The most common alleles are listed. [B]Individuals homozygous for *KIR3DS1* were excluded from the study and were therefore not included in the frequency calculation. Alleles with 47I are shown in red.

Supplemental Table 4: Effect of *KIR3DL1 I47V* on HIV control in *B*57+* individuals

3DL1 aa47	CTR N (%)	NC N (%)	OR adj.	*P* value
VV	91 (80.5)	48 (57.8)	0.2	$4x10^{-4}$
II	22 (19.5)	35 (42.2)		
IV	75 (77.3)	53 (60.2)	0.5	0.04
II	22 (22.7)	35 (39.8)		
VV	91 (54.8)	48 (47.5)	0.8	ns
IV	75 (45.2)	53 (52.5)		

Only individuals with 2 copies of KIR3DL1 were included in the analysis. Individuals with *3DL1/3DS1, 3DS1/3DS1, 3DL1*004* (1 or 2 copies), and *3DL1/-* were excluded.
CTR = controllers; NC = non-controllers; OR adj. = odds ratio adjusted by race; ns = not significant.

Supplemental Table 5: SPR-based equilibrium (K_D) values (μM) and standard errors for KIR3DL1-pHLA-B*57:01 interaction

Peptide	3DL1*001	3DL1*005	3DL1*015
IW9	16.7 ± 2.4	7.66 ± 0.8	21.3 ±3.1
KF11	34.6 ± 3.6	22.5 ± 2.1	49.3 ± 8.1
LF9	9.70 ± 0.4	4.29 ± 0.3	7.53 ± 1.2
QW9	21.8 ± 2.5	15.6 ± 1.2	25.8 ± 2.7

Supplemental Table 6: Relative effects of KIR3DL1 aa47, KIR3DS1 and KIR3DL1 expression level on HIV viremia[A].

Genotype	N	Effect (linear estimate)	SE	p value
B*57:01	398			
KIR3DL1 aa47 (per each additional aa47V)		-0.53	0.03	9×10^{-86}
KIR3DS1 (presence vs. absence)		-0.49	0.12	5×10^{-5}
KIR3DL1 expression level (h*/y vs. l/*x)[B]		-0.36	0.04	1×10^{-18}
B*57:03[C]	245			
KIR3DL1 aa47 (per each additional aa47V)		0.12	0.04	7×10^{-4}
KIR3DL1 expression level (h/*y vs. l/*x)[B]		0.25	0.05	6×10^{-7}

[A]Results are from a multivariate mixed linear effects model in individuals carrying one or more *HLA-B*57* alleles fitting the effect of the variable shown against longitudinal $\log_{10}$HIV VL. *HLA-A, -B* and *-C* alleles, and timing of viral load measurements were taken into account by being coded as random effects for all analyses.

[B]*KIR3DL1*h*/y* = individuals who carry a high expressing *KIR3DL1* allele (*KIR3DL1*h,* see Supplementary Figure 2) in the absence of a low expressing *KIR3DL1* allele (*KIR3DL1*l)*, i.e. *KIR3DL1*h/*h* or *KIR3DL1*h/*004*; abbreviated as *h/*y*, where **y* = **h* or **004*. *KIR3DL1*l/*y* = individuals with at least one copy of *KIR3DL1*l* (*KIR3DL1*l/*l*, *KIR3DL1*l/*h*, or *KIR3DL1*l/*004;* abbreviated as *l/*x*, where **x*= **l*, **h*, or **004* (27).

[C]Due to insufficient data, no results were generated for *KIR3DS1* (presence/absence).

Supplemental Figure Legends

Supplemental Figure 1: Manhattan plot of whole genome sequencing data derived from 100 B*57+ HIV controllers and 100 B*57+ noncontrollers. p-values are shown for 56,808 data points for all functional variants that were tested in Table 1 (WGS analysis). A single SNP on chromosome 17 (rs643347) exceeded the threshold for statistical significance defined by $p < 8.8 \times 10^{-7}$ after correcting for multiple comparisons.

Supplemental Figure 2: Allele frequency of the most common *KIR3DL1* alleles in the *HLA-B*57* study cohort. The frequency of each variable is shown for Whites and Blacks. Individuals homozygous for *KIR3DS1* were excluded from the study and were therefore not included in the frequency calculation. Alleles with 47I are shown in red and those with 47V in black. h = high cell surface expression alleles; l = low cell surface expression alleles; no = no cell surface expression.

Supplemental Figure 3: KIR3DL1 polymorphism affects binding avidity: (a) Cartoon representation of the KIR3DL1*001-HLA-B*57:01-LF9 ternary complex. KIR3DL1*001 (D0 domain gold, D1 domain green, D2 domain pink), HLA-B*57:01 (blue), β2m (grey), the peptide (black). The polymorphisms that distinguish KIR3DL1*015 (Val47 and Leu54) are shown as blue spheres. The N-terminus of KIR3DL1 did not extend beyond residue 6 (shown as *) in available crystal structures. Accordingly, the Met2Val substitution at position 2 is not

shown. The C-terminus of KIR3DL1 is labeled. The polymorphisms at positions 47 and 54 are modelled as forming a clustering interface with the α2 and α3 domains of an adjoining pHLA molecule, as observed in the crystallographic arrangement of molecules of the KIR3DL1-B*57:01 complex (33). (b-e) SPR-based affinity measurements of the interaction between KIR3DL1*001 (blue line), KIR3DL1*005 (red line), KIR3DL1*015 (green line) and their HLA B*57:01 ligand in complex with the IW9 (ISPRTLNAW) peptide (b), the KF11 (KAFSPEVIPMF) peptide (c), the LF9 (LSSPVTKSF) peptide (d) and the QW9 (QASQEVKNW) peptide (e). All data are for experiments performed in duplicate, from two independent experiments. Data are shown as mean ± standard deviation.

Supplemental Figure 1

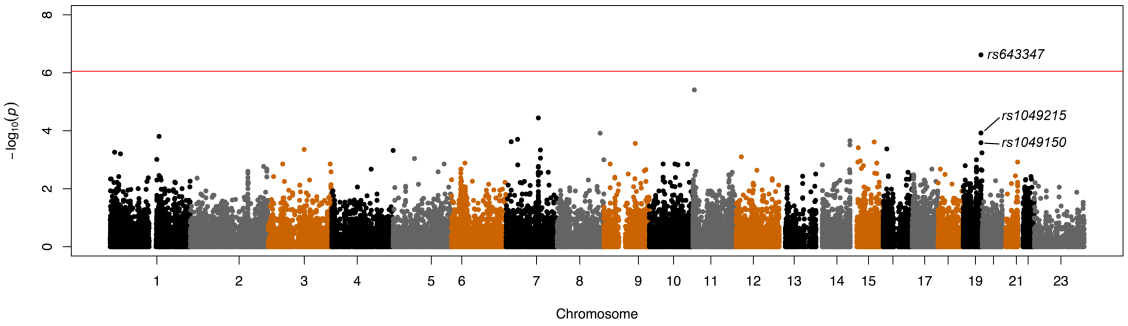

Supplemental Figure 1: Manhattan plot of whole genome sequencing data derived from 100 B*57+ HIV controllers and 100 B*57+ noncontrollers. p-values are shown for 56,808 data points for all functional variants that were tested in Table 1 (WGS analysis). A single SNP on chromosome 17 (rs643347) exceeded the threshold for statistical significance defined by $p < 8.8 \times 10^{-7}$ after correcting for multiple comparisons.

Supplemental Figure 2

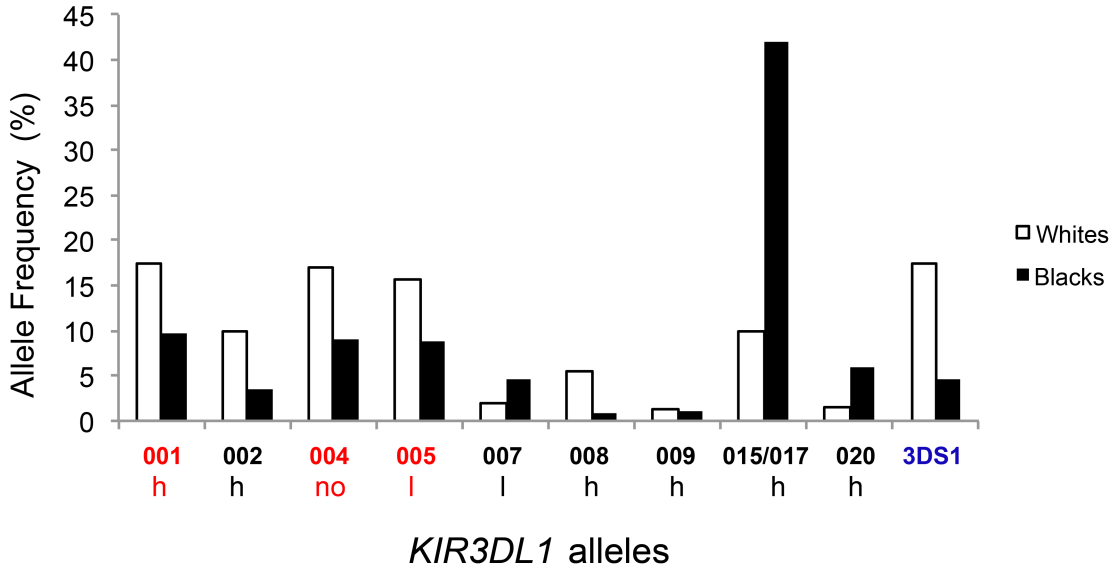

Supplemental Figure 2: Allele frequency of the most common *KIR3DL1* alleles in the *HLA-B*57* study cohort. The frequency of each variable is shown for Whites and Blacks. Individuals homozygous for *KIR3DS1* were excluded from the study and were therefore not included in the frequency calculation. Alleles with 47I are shown in red and those with 47V in black. h = high cell surface expression alleles; l = low cell surface expression alleles; no = no cell surface expression.

Supplemental Figure 3

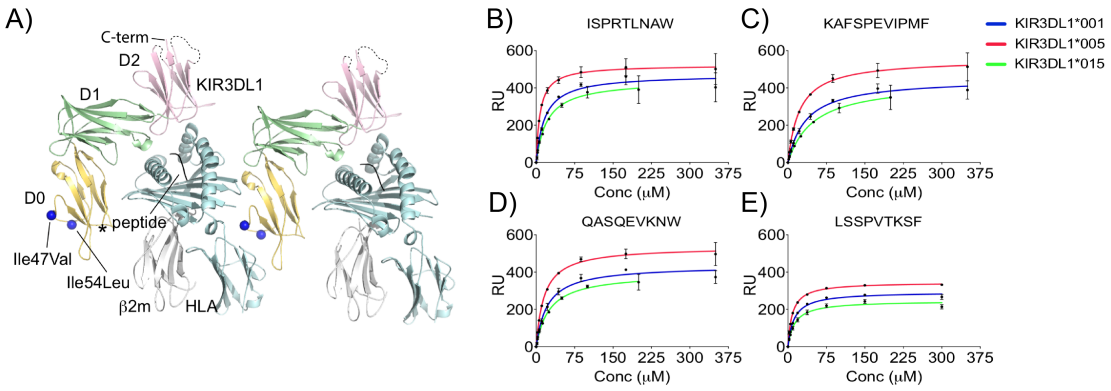

Supplemental Figure 3: KIR3DL1 polymorphism affects binding avidity: (a) Cartoon representation of the KIR3DL1*001-HLA-B*57:01-LF9 ternary complex. KIR3DL1*001 (D0 domain gold, D1 domain green, D2 domain pink), HLA-B*57:01 (blue), β2m (grey), the peptide (black). The polymorphisms that distinguish KIR3DL1*015 (Val47 and Leu54) are shown as blue spheres. The N-terminus of KIR3DL1 did not extend beyond residue 6 (shown as *) in available crystal structures. Accordingly, the Met2Val substitution at position 2 is not shown. The C-terminus of KIR3DL1 is labeled. The polymorphisms at positions 47 and 54 are modelled as forming a clustering interface with the α2 and α3 domains of an adjoining pHLA molecule, as observed in the crystallographic arrangement of molecules of the KIR3DL1-B*57:01 complex (33). (b-e) SPR-based affinity measurements of the interaction between KIR3DL1*001 (blue line), KIR3DL1*005 (red line), KIR3DL1*015 (green line) and their HLA B*57:01 ligand in complex with the IW9 (ISPRTLNAW) peptide (b), the KF11 (KAFSPEVIPMF) peptide (c), the LF9 (LSSPVTKSF) peptide (d) and the QW9 (QASQEVKNW)

peptide (e). All data are for experiments performed in duplicate, from two independent experiments. Data are shown as mean ± standard deviation.